IMPERIAL

Statistical Methods in Finance Project

Imperial College London

Department of Mathematics

Nonparametric Pricing of Exotic Derivatives via Implied Expected Signature

Authors:
Arthur Nageleisen (CID 06058657)
Christopher Dybdahl (CID 06060098)
Kutay Mendi (CID 06055947)
Luca Würker (CID 06059154)

Date: January 19, 2026

Contents

1 Introduction

Classical derivative pricing typically commits to a parametric model for the asset dynamics and then prices by expectation under a risk-neutral measure. For exotic (path-dependent) options, this can be fragile due to issues such as model misspecification, unstable calibration, and difficulty capturing the path features that actually matter for the payoff.

Lyons et al. [2019a] propose a model-free approach built around a universal set of path features, the (rough path) signature. A key result is that many path-dependent payoffs can be well-approximated by linear functionals of a truncated signature. This motivates a corresponding family of primitive 'building blocks' called signature payoffs. These intend to serve for path-dependent claims what Arrow–Debreu securities Arrow [1973], Debreu [1987] serve for state-contingent claims.

In practice, the market's risk-neutral law on path space is not directly observable. The authors therefore compress the relevant pricing information into an implied expected signature. This is the (risk-neutral) expected truncated signature that best matches observed market prices from a sufficiently rich basket of traded (vanilla and exotic) derivatives. Once inferred (essentially via a regression-style calibration), it can be used to price new exotic payoffs out-of-sample. We show that performance is strong when the calibration set includes diverse exotics and weaker when using vanillas alone.

2 Theoretical groundwork

We denote the extended tensor algebra over $\mathbb{R}^d$ by $T((\mathbb{R}^d))$ and the signature of a path Z truncated at order N by $\mathrm{Sig}^N(Z)$. Formal definitions (tensor algebra and iterated integrals) are given in Appendix A. The signature of a path is an infinite sequence of tensors (1, level-1, level-2, ...). After truncation it becomes a finite feature vector, so path-functionals can be approximated by linear forms $\langle \ell, \mathrm{Sig}^N(\cdot)\rangle$ and pricing/hedging reduces to finite-dimensional linear algebra.

2.1 Market Framework

Following Lyons et al. [2019a], fix trading times $\mathbb{T} = \{t_i\}_{i=0}^n \subset [0,1]$ with $0 = t_0 < \cdots < t_n = 1$, and consider a single risky asset with *discounted* price paths $\Omega := \{X : \mathbb{T} \to \mathbb{R}_+ : X_0 = 1\}$.

For technical reasons (see below) we lift the discrete price path $X \in \Omega$ to a continuous curve via the *lead–lag transformation*. We define $\widehat{X} : [0,1] \to \mathbb{R}^2 \oplus \mathbb{R}$ by linear interpolation between the nodes

$$\widehat{X}_{2k/2n} := \Big((t_k, X_{t_k}), X_{t_k}\Big) \in \mathbb{R}^2 \oplus \mathbb{R}, \quad \text{and} \quad \widehat{X}_{(2k+1)/2n} := \Big((t_k, X_{t_k}), X_{t_{k+1}}\Big) \in \mathbb{R}^2 \oplus \mathbb{R}.$$

We write $\widehat{X}_t = (X_t^b, X_t^f)$ where $X_t^b \in \mathbb{R}^2$ denotes the *lag* (backward) component and $X_t^f \in \mathbb{R}$ denotes the *lead* (forward) component. We define the space of lead–lag price paths $\widehat{\Omega} := \{\widehat{X} : X \in \Omega\}$.

While the signature of a raw 1D price path generally does not uniquely identify the path, this transformation restores injectivity, as established by the following result:

Lemma 1 (Uniqueness of signature, Hambly and Lyons [2010])
The signature map $\mathrm{Sig} : \widehat{\Omega} \to T((\mathbb{R}^2 \oplus \mathbb{R}))$ *is injective.*

To illustrate, consider the paths $A_t \equiv 0$ and $B_t = 1 - |t-1|$ on $[0,2]$. In one dimension the signature depends only on total increment (terms $(Z_T - Z_0)^n/n!$), so both have signature $(1, 0, \dots)$ and the volatility of B is invisible. The lead-lag transform $\widehat{Z}$ resolves this by lifting the paths to $\mathbb{R}^2$ Flint et al. [2016] [1]. Specifically, the second-level Lévy area Lyons et al. [2007],

$$\mathcal{A}(\widehat{Z}) = \frac{1}{2}\int_0^2 (Z^b\, dZ^f - Z^f\, dZ^b), \tag{1}$$

distinguishes the two. We have $\mathcal{A}(\widehat{A}) = 0$, whereas $\widehat{B}$ traces a loop with $\mathcal{A}(\widehat{B}) = 1$, This antisymmetric second-level term measures the signed area traced by the lead–lag path in the plane (see Figure 1), and is closely linked to quadratic variation in the semimartingale setting.

[1] In our definition of lead-lag transform we augment the path with a time t coordinate, mapping to $\mathbb{R}^2 \oplus \mathbb{R}$. However for this

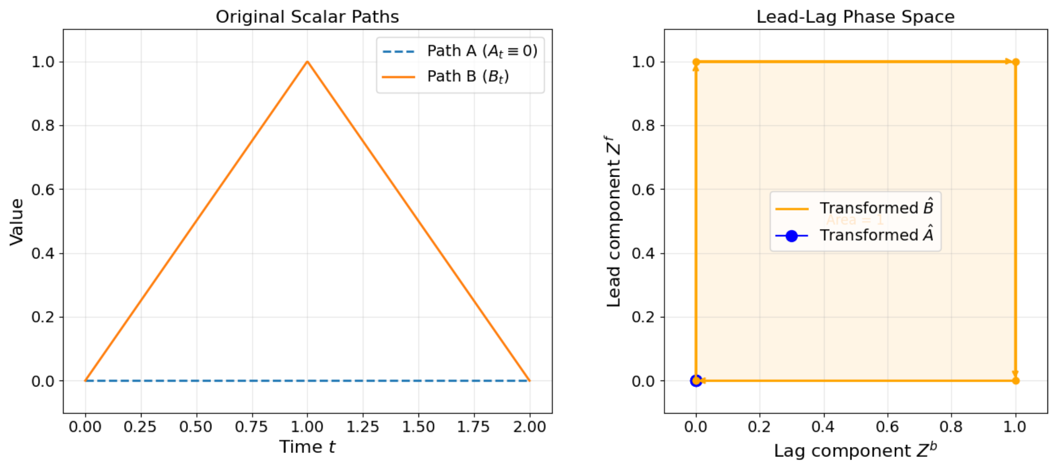

Figure 1: Visualization of the Lead–Lag transformation. The volatile path (orange) forms a loop in the phase portrait (right) whose geometric area captures quadratic variation, distinguishing it from the zero-area flat path (blue)

2.2 Signature Payoffs

With these preliminaries in place, we formulate the pricing problem. Payoffs are defined as measurable functions $G : \widehat{\Omega} \to \mathbb{R}$. The paper assumes a nonempty, tight set of risk-neutral measures $\mathcal{M}$ on $\widehat{\Omega}$, and defines the pricing map

$$\mathcal{P}(G) := \sup_{\mathbb{Q}\in\mathcal{M}} E^{\mathbb{Q}}[G(\widehat{X})].$$

Here we work with discounted payoffs/prices and discard an explicit discount factor. Let $\mathcal{F} = \{F_i\}_{i=1}^{m}$ be a finite family of traded payoffs available at $t = 0$ (later used as the calibration set). By construction, $\mathcal{M}$ is chosen to match their observed market prices, i.e.

$$\mathbb{E}^{\mathbb{Q}}[F_i(\widehat{X})] = \mathcal{P}(F_i) \qquad \text{for all } i = 1, \dots, m \text{ and all } \mathbb{Q} \in \mathcal{M}.$$

Hence, for any $F \in \mathcal{F}$, the map $\mathbb{Q} \mapsto \mathbb{E}^{\mathbb{Q}}[F(\widehat{X})]$ is constant on $\mathcal{M}$, and therefore $\mathcal{P}(F) = \mathbb{E}^{\mathbb{Q}}[F(\widehat{X})] \quad \forall \mathbb{Q} \in \mathcal{M}$.
For a general exotic payoff $G \notin \mathcal{F}$, calibration alone does not pin down a unique expectation, and we therefore retain the robust definition $P(G) = \sup_{\mathbb{Q}\in\mathcal{M}} \mathbb{E}^{\mathbb{Q}}[G(\widehat{X})]$.
To render this framework computationally tractable Lyons et al. [2019a] introduce signature payoffs as 'primitive' path-dependent securities. A signature payoff is defined as a linear functional applied to the signature of the (lead–lag transformed) path:

$$S_\ell(\widehat{X}) := \langle \ell, \mathrm{Sig}(\widehat{X})_{0,1} \rangle, \qquad \widehat{X} \in \widehat{\Omega} \qquad \ell \in T((\mathbb{R}^2 \oplus \mathbb{R})^*).$$

Thus S_ℓ is a linear combination of iterated integrals of the path. The theoretical justification for using these payoffs is a density/approximation result: broad classes of continuous path-dependent payoffs can be approximated (on compacts) by linear functionals of a truncated signature. The main result supporting this methodology is:

Proposition 1. Local uniform approximation on compacts. (Proposition 4.2 in Lyons et al. [2019a])
Let $G : \widehat{\Omega} \to \mathbb{R}$ be a continuous payoff and let $K \subset \widehat{\Omega}$ be compact. For any $\varepsilon > 0$, there exists a signature payoff S_ℓ with $\ell \in T((\mathbb{R}^2 \oplus \mathbb{R})^*)$ such that

$$|G(\widehat{X}) - S_\ell(\widehat{X})| = |G(\widehat{X}) - \langle \ell, \mathrm{Sig}(\widehat{X}) \rangle| < \varepsilon, \qquad \forall \widehat{X} \in K.$$

While Proposition 1 establishes uniform approximation on fixed compacts, the authors relax this into a probabilistic statement. They use the tightness of $\mathcal{M}$ to choose (for each ε) a high-probability compact set $K_\varepsilon \subset \widehat{\Omega}$ ($\mathbb{Q}(K_\varepsilon) \geq 1 - \varepsilon$) such that there exists signature payoff S_ℓ that matches the payoff G with small error on K_ε.

illustration augmentation is no required because the 'separation' we are looking for already occurs in the $(\widehat{Z}^b, \widehat{Z}^f)$ coordinates.

This functional approximation directly implies pricing accuracy. Since derivative prices are simply discounted risk-neutral expectations, replacing G with the nearby signature payoff S_ℓ on this high-probability set yields a minimal pricing error. Consequently, provided the family is integrable, $\mathbb{E}^{\mathbb{Q}}[G(\widehat{X})] \approx \mathbb{E}^{\mathbb{Q}}[S_\ell(\widehat{X})]$, demonstrating that signatures are not only dense for *functions* on path space, but also provide accurate *prices* once expectations are taken (**Proposition 4.4** in Lyons et al. [2019a]).

2.3 Implied Expected Signature

This leads us to the concept of the implied expected signature. Fix $\varepsilon > 0$. The paper then *extends* **Proposition 4.4** in Lyons et al. [2019a] to a family of payoffs. Concretely, one can choose a compact set $K_\varepsilon \subset \widehat{\Omega}$ and, for each traded payoff F in a chosen family $\mathcal{F}$, a coefficient ℓ_F such that $\mathbf{1}_{K_\varepsilon} S_{\ell_F}$ is close to F in the robust pricing sense

$$\mathcal{P}\Big(|F - \mathbf{1}_{K_\varepsilon} S_{\ell_F}|\Big) = \sup_{\mathbb{Q}\in\mathcal{M}} \mathbb{E}^{\mathbb{Q}}\Big[|F(\widehat{X}) - \mathbf{1}_{K_\varepsilon} S_{\ell_F}(\widehat{X})|\Big] < \varepsilon \qquad \text{while also} \qquad \mathbb{Q}(X \in K_\varepsilon) > 1-\varepsilon \quad \text{for all } \mathbb{Q}\in\mathcal{M}.$$

Now fix a single risk-neutral measure $\mathbb{Q} \in \mathcal{M}$. Since $S_{\ell_F}(X) = \langle \ell_F, \mathrm{Sig}(X)_{0,1}\rangle$, and truncating at level N (for N large enough) gives

$$\mathcal{P}(F) = \mathbb{E}^{\mathbb{Q}}[F(\widehat{X})] \;\approx\; \mathbb{E}^{\mathbb{Q}}\Big[\mathbf{1}_{K_\varepsilon} S_{\ell_F}(\widehat{X})\Big] = \mathbb{E}^{\mathbb{Q}}\Big[\mathbf{1}_{K_\varepsilon}\langle \ell_F, \mathrm{Sig}(\widehat{X})_{0,1}\rangle\Big] \;\approx\; \mathbb{E}^{\mathbb{Q}}\Big[\mathbf{1}_{K_\varepsilon}\langle \ell_F, \mathrm{Sig}^N(\widehat{X})_{0,1}\rangle\Big], \qquad \forall F \in \mathcal{F}.$$

Hence by linearity of the expectation, $\mathcal{P}(F) \;\approx\; \Big\langle \ell_F,\, \mathbb{E}^{\mathbb{Q}}\Big[\mathrm{Sig}^N(\widehat{X})_{0,1}\,\mathbf{1}_{K_\varepsilon}\Big]\Big\rangle, \forall F \in \mathcal{F}$.

As the above relation holds for all contracts in $\mathcal{F}$, even if the risk-neutral measures are unknown but we observe market prices for the exotic payoffs $\mathcal{F}$, we should be able to find an implied expected signature $\mathbf{E}$ that best matches the observed prices. This is analogous to the concept of implied volatility in the BS framework. Essentially we just replace $\mathbb{E}^{\mathbb{Q}}\Big[\mathrm{Sig}^N(\widehat{X})_{0,1}\,\mathbf{1}_{K_\varepsilon}\Big]$ with some $\mathbf{E} \in T^{(N)}(\mathbb{R}^2 \oplus \mathbb{R})$ in the above approximate equality.

The quality (and identifiability) of the implied expected signature E depends on how "rich" the calibration set $\mathcal{F}$ is. After truncation at level N, $\mathbf{E} \in T^{(N)}(\mathbb{R}^2 \oplus \mathbb{R})$ is finite-dimensional, and each traded payoff $F \in \mathcal{F}$ provides an (approximate) linear constraint $\mathcal{P}(F) \approx \langle \ell_F, \mathbf{E}\rangle$. These constraints determine $\mathbf{E}$ only if the coefficient vectors $\{\ell_F\}_{F\in\mathcal{F}}$ span (or nearly span) the relevant subspace of $T^{(N)}$. If $\mathcal{F}$ is not rich enough, the resulting regression becomes ill-conditioned because many different $\mathbf{E}$'s fit the same observed prices almost equally well. In other words, the calibration map $\mathbf{E} \mapsto \big(\langle \ell_F, \mathbf{E}\rangle\big)_{F\in\mathcal{F}}$ is nearly non-injective. This is exactly the same instability as multicollinearity in linear regression, where highly dependent predictors make the fitted coefficients unstable.

3 Numerical Implementation

We implement the pricing procedure of Lyons–Nejad–Perez Arribas (2020): learn signature-linear approximations of payoffs, infer an implied expected signature from calibration prices, then price new exotics by a dot product.

Data and benchmark prices. We focus on the S&P 500 Index (SPX). European option prices across a grid of strikes (Bloomberg) provide liquid vanilla inputs. Since traded SPX exotics are typically OTC and not publicly observable, we generate benchmark ("true") prices for Asian calls, up-and-in barrier calls, and up-and-out barrier calls by Monte Carlo under several market generators: GBM, jump diffusion, stochastic volatility (Heston), and rough volatility.

Why multiple market generators. The implied expected signature is intended to be a nonparametric summary of risk-neutral path dynamics (up to truncation), so performance should not depend on any single parametric model. Although GBM paths are used in Step (1) to learn payoff coefficients ℓ_i, out-of-sample pricing is evaluated under distinct generators to demonstrate robustness beyond the training model.

3.1 Algorithm

Step (1): We first simulate sample paths $\{\widehat{X}^{(j)}\}_{j=1}^{n}$ on a time grid over maturity T using a GBM model with varying volatilities. After applying a lead–lag transform to compute truncated signatures $\mathrm{Sig}^N(\widehat{X}^{(j)})$ for $N = 5$, we fit coefficients ℓ_i via linear regression such that $\langle \ell_i, \mathrm{Sig}^N(\widehat{X}^{(j)})\rangle \approx F_i(\hat{X}^{(j)})$ for all paths j. This produces a coefficient vector ℓ_i for each traded payoff (i.e. an explicit signature–payoff approximation S_{ℓ_i} for F_i).

Step (2): Let p_i be the observed market price of payoff $F_i \in \mathcal{F}$ at $t = 0$. For signature-linear payoffs, pricing is linear in the expected signature, so the paper's motivating relation is $p_i \approx \langle \ell_i, s\rangle$ where s denotes the (discounted) implied expected truncated signature. Stacking across $i = 1, \dots, m$ gives a linear inverse problem

$$p \approx As, \qquad A := \begin{pmatrix} \ell_1^\top \\ \vdots \\ \ell_m^\top \end{pmatrix}, \qquad p := (p_1, \dots, p_m)^\top.$$

We then solve for s using least squares: $\hat{s} = \arg\min_s \|As - p\|^2$.

Step (3): For each test payoff G_k not used in calibration, we first learn ℓ_{G_k} as in Step 1, then predict its price by $\hat{\mathcal{P}}(G_k) = \langle \ell_{G_k}, \hat{s}\rangle$.

We compare $\hat{\mathcal{P}}(G_k)$ to benchmark "market prices" and report R^2 and pricing errors.

3.2 Out-of-sample pricing test

For each market generator we price four payoff families—European calls, Asian calls, up-and-out barrier calls and up-and-in barrier calls—each on the same grid of 50 strikes (25-point spacing) around S_0. This gives $m_{\text{tot}} = 200$ contracts per model. We split *by contract* using a 50/50 split within each family: 25 strikes per family (100 contracts) are used for calibration (Step (2)) and the remaining 100 are held out for out-of-sample pricing (Step (3)).

We implement Steps (1)–(3) (see Laloi Dybdahl et al. [2026]) on synthetic markets and, where available, on SPX vanilla data. In synthetic environments we obtain very high R^2 (Figures 2a–2c), consistent with Lyons et al. [2019a]. On real SPX calls/puts the fit is weaker, plausibly due to market frictions (bid–ask, discreteness, stale quotes, liquidity premia) and, more fundamentally, because vanillas alone do not provide the "rich" calibration set of path-dependent exotics needed to identify the signature directions relevant for exotic pricing (Section 2).

3.3 Multi-Asset Extensions

The same theoretical framework extends to multiple assets Lyons et al. [2019b]. For d discounted assets $X^{(1)}, \dots, X^{(d)}$, apply the lead–lag lift to the joint path $(t, X_t^{(1)}, \dots, X_t^{(d)})$. The truncated signature then contains cross-terms that encode inter-asset dependence. In the semimartingale case, level-2 cross-terms are closely related to quadratic covariation. The numerical pipeline (1)–(3) is unchanged, but identification is harder. Single-asset vanillas alone may not pin down the cross-asset directions in the implied expected signature. directions of the implied expected signature. A practical calibration set would therefore include basket/spread vanillas and multi-asset exotics (e.g. barrier- or path-dependent structures). Since such quotes are typically OTC and scarce, empirical validation would likely rely on synthetic markets (e.g. correlated GBM/Heston or multivariate GARCH) unless proprietary data are available.

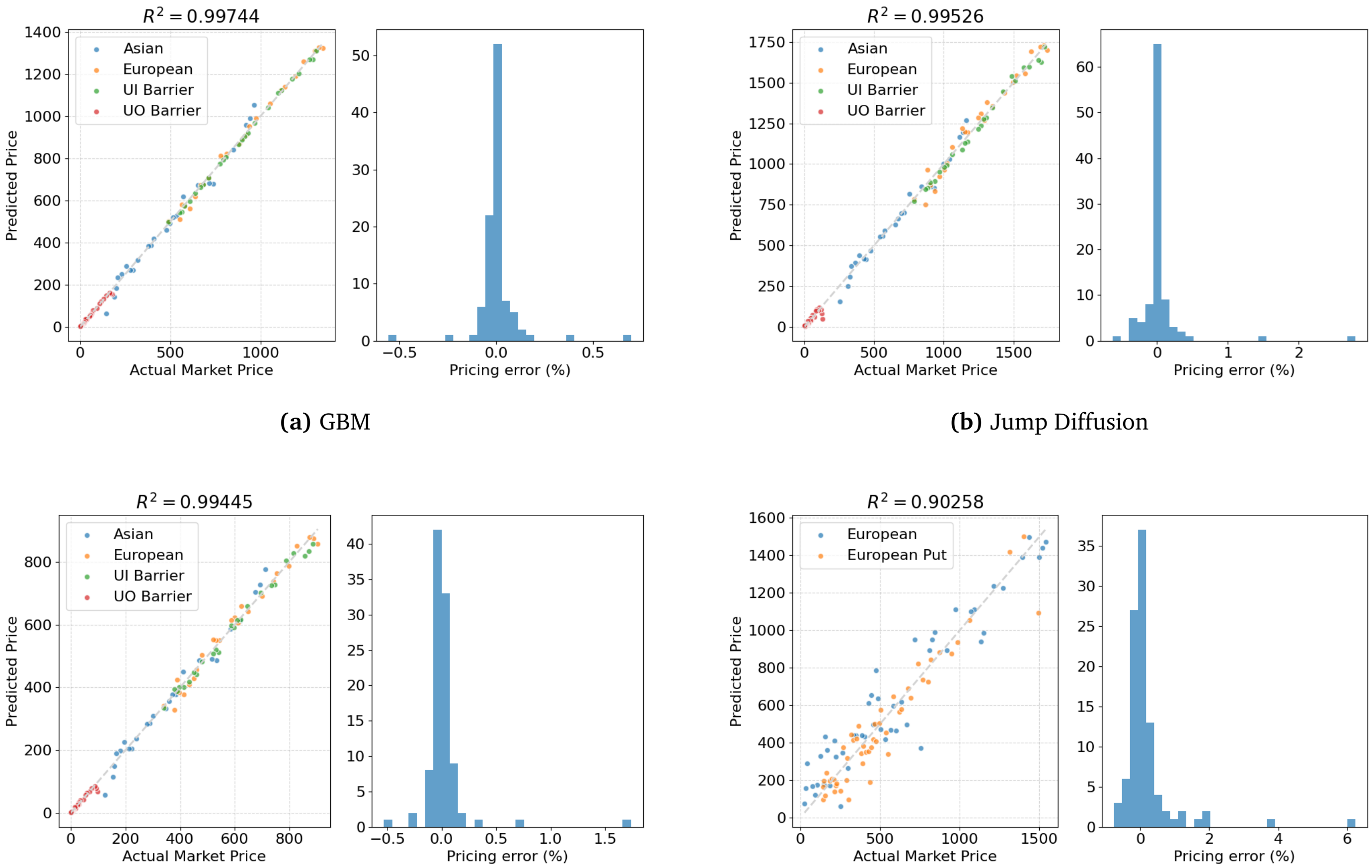

(a) GBM

(b) Jump Diffusion

(c) Rough Volatility

(d) Real SPX Prices

Figure 2: Model pricing and calibration results

4 Conclusion and Critique

We implemented and reviewed the nonparametric pricing framework of Lyons, Nejad and Perez Arribas Lyons et al. [2019a], which infers an implied expected signature from calibration prices and then prices new exotics by linear evaluation. In synthetic markets we replicate the paper's high out-of-sample accuracy, and we additionally find robustness under Jump Diffusion dynamics. Crucially, we confirm that the linear functional approximation for payoffs can be effectively learned using 'simple' GBM training paths, yet successfully generalise to price under complex, distinct market dynamics. This supports the 'model-free' intent of the method.

Two practical limitations stand out. First, reproducibility is hindered by sparse implementation details in the literature, which makes independent verification harder than it needs to be. This serves as a bottleneck for further academic development and industrial adoption. Second, data availability is a binding constraint. Identification relies on a sufficiently rich, liquid calibration set $\mathcal{F}$, yet the most informative path-dependent exotics are typically OTC with non-public and non-synchronised quotes. As a result, while the framework provides a compelling unification of prices in principle, its real-world deployment is currently restricted to settings with access to proprietary exotic pricing data.

The framework also rests on simplifying assumptions. It is frictionless, so pricing conclusions do not directly reflect transaction costs, bid–ask spreads, or liquidity effects (treated theoretically in Lyons et al. [2019b] but not implemented numerically in the 2020 study). Truncation is another structural trade-off. The dimension of $T^{(N)}(\mathbb{R}^2 \oplus \mathbb{R})$ grows exponentially with N, so feasible choices of N may miss payoff-relevant path information. The authors could have studied the effect of size of N in their approach, which could easily ve implemented by systematic sensitivity analysis of outcomes with respect to N. Finally, numerical tests largely focus on standard Asians and barriers, and do not stress highly structured exotics (e.g. autocallables, cliquets, ratchets, coupon features, or multi-asset hybrids), where both approximation and identification may be harder.

A Mathematical Preliminaries

In this appendix, we formalize the algebraic space in which signatures reside and define the signature map as an iterated-integral feature for paths.

A.1 Tensor Algebra

Fix $d \geq 1$. For $n \in \mathbb{N}$, let $(\mathbb{R}^d)^{\otimes n}$ denote the n-fold tensor product, with the convention $(\mathbb{R}^d)^{\otimes 0} := \mathbb{R}$. We define the extended tensor algebra over $\mathbb{R}^d$ and its truncation of order N respectively as:

$$T((\mathbb{R}^d)) := \prod_{n=0}^{\infty} (\mathbb{R}^d)^{\otimes n} \qquad \text{and} \qquad T^{(N)}(\mathbb{R}^d) := \prod_{n=0}^{N} (\mathbb{R}^d)^{\otimes n}. \tag{2}$$

We utilize the natural bilinear pairing between tensors and their duals. For a linear functional $\ell = (\ell_0, \ell_1, \dots) \in T((\mathbb{R}^d))^*$ and an element $a = (a_0, a_1, \dots) \in T((\mathbb{R}^d))$, the pairing is defined as:

$$\langle \ell, a \rangle := \sum_{n=0}^{\infty} \langle \ell_n, a_n \rangle,$$

whenever this series is well-defined. For truncated objects in $T^{(N)}(\mathbb{R}^d)$, this sum is finite and always well-defined.

A.2 Signature of a Path

Let $Z : [0, T] \to \mathbb{R}^d$ be a sufficiently regular path (e.g., of bounded variation or a geometric rough path). The signature of Z over the interval $[s, t]$ is given by the sequence:

$$\mathrm{Sig}(Z)_{s,t} = (1, Z^1_{s,t}, Z^2_{s,t}, \dots) \in T((\mathbb{R}^d)), \tag{3}$$

where the n-th level term $Z^n_{s,t}$ is defined by the iterated integral:

$$Z^n_{s,t} := \int_{s<u_1<\cdots<u_n<t} dZ_{u_1} \otimes \cdots \otimes dZ_{u_n}. \tag{4}$$

The truncated signature at level N, denoted by $\mathrm{Sig}^N(Z)_{s,t}$, is obtained by projecting the full signature onto the truncated space $T^{(N)}(\mathbb{R}^d)$.

For a given truncation order N, the number of raw signature coordinates for a d-dimensional path grows geometrically:

$$\dim T^{(N)}(\mathbb{R}^d) = 1 + d + d^2 + \cdots + d^N = \frac{d^{N+1} - 1}{d - 1}.$$

This is why truncation is essential in practice.

References

Terry Lyons, Sina Nejad, and Imanol Perez Arribas. Numerical method for model-free pricing of exotic derivatives in discrete time using rough path signatures. **Applied Mathematical Finance**, 26(6), 2019a. doi: 10.1080/1350486X.2020.1726784. URL `https://doi.org/10.1080/1350486X.2020.1726784`. pages 1, 2, 3, 4, 5

Kenneth J. Arrow. **Essays in the Theory of Risk-Bearing**. North-Holland, Amsterdam, 1973. pages 1

Gerard Debreu. **Theory of Value: An Axiomatic Analysis of Economic Equilibrium**. Yale University Press, New Haven, 1987. pages 1

Ben Hambly and Terry Lyons. Uniqueness for the signature of a path of bounded variation and the reduced path group. **Annals of Mathematics**, 171(1), 2010. doi: 10.4007/annals.2010.171.109. pages 1

G. Flint, B. Hambly, and T. Lyons. Discretely sampled signals and the rough hoff process. **Stochastic Processes and their Applications**, 126(9), 2016. doi: 10.1016/j.spa.2016.02.011. pages 1

Terry J. Lyons, Michael Caruana, and Thierry Lévy. **Differential Equations Driven by Rough Paths**, volume 1908 of **Lecture Notes in Mathematics**. Springer Berlin Heidelberg, Berlin, Heidelberg, 2007. pages 1

Christopher Laloi Dybdahl, Arthur Nageleisen, Kutay Mendi, and Luca Wurker. Numerical methods for rough path signatures. `https://github.com/christopher-dybdahl/rough-path-signatures-pricing`, 2026. GitHub repository, accessed 17 January 2026. pages 4

Terry Lyons, Sina Nejad, and Imanol Perez Arribas. Nonparametric pricing and hedging of exotic derivatives. arXiv preprint arXiv:1905.00711, 2019b. Submitted May 2 2019. pages 4, 5